

## Accelerated Publications

---

### Structural Basis of Electron Transfer Modulation in the Purple Cu<sub>A</sub> Center<sup>†</sup>

Howard Robinson,<sup>‡</sup> Marjorie C. Ang,<sup>§</sup> Yi-Gui Gao,<sup>‡</sup> Michael T. Hay,<sup>§</sup> Yi Lu,<sup>\*,§</sup> and Andrew H.-J. Wang<sup>\*,‡,§</sup>

Department of Cell and Structural Biology and Department of Chemistry, University of Illinois at Urbana-Champaign, Urbana, Illinois 61801

Received January 22, 1999; Revised Manuscript Received March 8, 1999

**ABSTRACT:** The X-ray structure of an engineered purple Cu<sub>A</sub> center in azurin from *Pseudomonas aeruginosa* has been determined and refined at 1.65 Å resolution. Two independent purple Cu<sub>A</sub> azurin molecules are in the asymmetric unit of a new *P*2<sub>1</sub> crystal, and they have nearly identical conformations (rmsd of 0.27 Å for backbone atoms). The purple Cu<sub>A</sub> azurin was produced by the loop-engineering strategy, and the resulting overall structure is unperturbed. The insertion of a slightly larger Cu-binding loop into azurin causes the two structural domains of azurin to move away from each other. The high-resolution structure reveals the detailed environment of the delocalized mixed-valence [Cu(1.5)•••Cu(1.5)] binuclear purple Cu<sub>A</sub> center, which serves as a useful reference model for other native proteins, and provides a firm basis for understanding results from spectroscopic and functional studies of this class of copper center in biology. The two independent Cu–Cu distances of 2.42 and 2.35 Å (with respective concomitant adjustments of ligand–Cu distances) are consistent with that (2.39 Å) obtained from X-ray absorption spectroscopy with the same molecule, and are among the shortest Cu–Cu bonds observed to date in proteins or inorganic complexes. A comparison of the purple Cu<sub>A</sub> azurin structure with those of other Cu<sub>A</sub> centers reveals an important relationship between the angular position of the two His imidazole rings with respect to the Cu<sub>2</sub>S<sub>2</sub>(Cys) core plane and the distance between the Cu and the axial ligand. This relationship strongly suggests that the fine structural variation of different Cu<sub>A</sub> centers can be correlated with the angular positions of the two histidine rings because, from these positions, one can predict the relative axial ligand interactions, which are responsible for modulating the Cu–Cu distance and the electron transfer properties of the Cu<sub>A</sub> centers.

Purple Cu<sub>A</sub> centers, found in cytochrome *c* oxidase (COX) of eukaryotic mitochondria and some aerobic bacteria (1), and in nitrous oxide reductase (N<sub>2</sub>OR) of dinitrifying bacteria (2), are a new class of copper centers in biology. Like the classic blue (type 1) copper proteins (3, 4), they are involved

in long-range electron transfer (ET) (5, 6). However, rather than adopting the active site structure of the blue copper proteins that contains a mononuclear Cu(II) with one cysteine and two histidines in a trigonal plane (7), purple Cu<sub>A</sub> centers contain a mixed-valent binuclear [Cu(1.5)•••Cu(1.5)] center with one histidine bound to each copper and two cysteines serving as bridging ligands (8–11). Understanding the structure–function relationship of this class of copper centers has been the focus of intense research (12), including many excellent biochemical (13–15), spectroscopic (for example, see refs 16–28), and electron transfer (5, 6, 29–32) studies

<sup>†</sup> This work was supported by NIH Grant GM41612 to A.H.-J.W. and NSF Grant CHE-9502421 to Y.L. Y.L. is an Alfred P. Sloan Fellow, a Beckman Young Investigator of the Arnold and Mabel Beckman Foundation, and a Cottrell Scholar of the Research Corp.

\* To whom correspondence should be addressed.

<sup>‡</sup> Department of Cell and Structural Biology.

<sup>§</sup> Department of Chemistry.

on either the water-soluble fragments containing the Cu<sub>A</sub> center of native enzymes (33–35), engineered Cu<sub>A</sub> centers (36–38), or inorganic model compounds (39, 40). One central question is how the electron transfer function of purple Cu<sub>A</sub> centers is modulated with respect to those of blue copper centers.

To answer this question, we (37) and others (38) have succeeded in converting the blue copper center into the purple Cu<sub>A</sub> center using loop-directed mutagenesis. Comprehensive spectroscopic characterization of the engineered azurin from *Pseudomonas aeruginosa* (called purple Cu<sub>A</sub> azurin) has demonstrated the striking similarity between the purple Cu<sub>A</sub> azurin and the native Cu<sub>A</sub> centers (20, 37, 41–44). From the study, a correlation between the high-energy Cu–Cu  $\sigma \rightarrow \sigma^*$  transition and the Cu–Cu core compression was noted. A detailed investigation by Gamelin et al. (20), who used a combination of electronic spectroscopic characterization and molecular orbital calculations, demonstrated that both valence delocalization and the axial ligand interaction are important for modulation of the electronic structure and control of both ET redox potential and reorganization energy. It was proposed that the weakening of the axial ligand interaction can result in more Cu–Cu compression, stronger valence delocalization, and smaller reorganization energy, and therefore more efficient ET. A comparison with the electronic structural description of the blue copper centers indicates that weakened axial interactions also occur, although no valence delocalization can be operative in the blue copper centers. More importantly, an ET study of the engineered purple Cu<sub>A</sub> azurin showed that, within the same protein framework and despite a  $\sim 70$  mV lower driving force, the mixed-valent purple Cu<sub>A</sub> center transfers an electron about 3 times faster than the blue copper center, which can be attributed to the lower reorganization energy of the Cu<sub>A</sub> center (45).

To provide a basis for understanding the results from both spectroscopic and ET studies, high-resolution structures containing different Cu–Cu and axial ligand–Cu distances are required. To date, three crystal structures of proteins containing the purple Cu<sub>A</sub> center, namely, COX from bovine heart (8, 9) and from *Paracoccus denitrificans* (10, 11) at 2.8 Å and quinol oxidase (CyoA) construct (46) at 2.3 Å, have established medium-resolution structures for the purple Cu<sub>A</sub> centers. Here we present the high-resolution structure of the engineered purple Cu<sub>A</sub> azurin determined by X-ray crystallography (Figure 1) from which the structure of the mixed-valence binuclear Cu<sub>2</sub>S<sub>2</sub>(Cys) core is defined in an unprecedentedly clear manner. This high-resolution structure allows us to correlate the structure with results from many spectroscopic studies, and to define structural elements that are important for modulation of the functional properties of the center. Furthermore, the purple Cu<sub>A</sub> azurin is engineered using loop-directed mutagenesis (37). In contrast to site-directed mutagenesis, loop-directed mutagenesis has been used only recently for protein engineering purposes (36–38). Therefore, understanding structural elements determining the success of loop-directed mutagenesis can help make this technique more applicable to other proteins.

## MATERIALS AND METHODS

The purple Cu<sub>A</sub> azurin was constructed and expressed in *Escherichia coli*, and the holoprotein was purified to

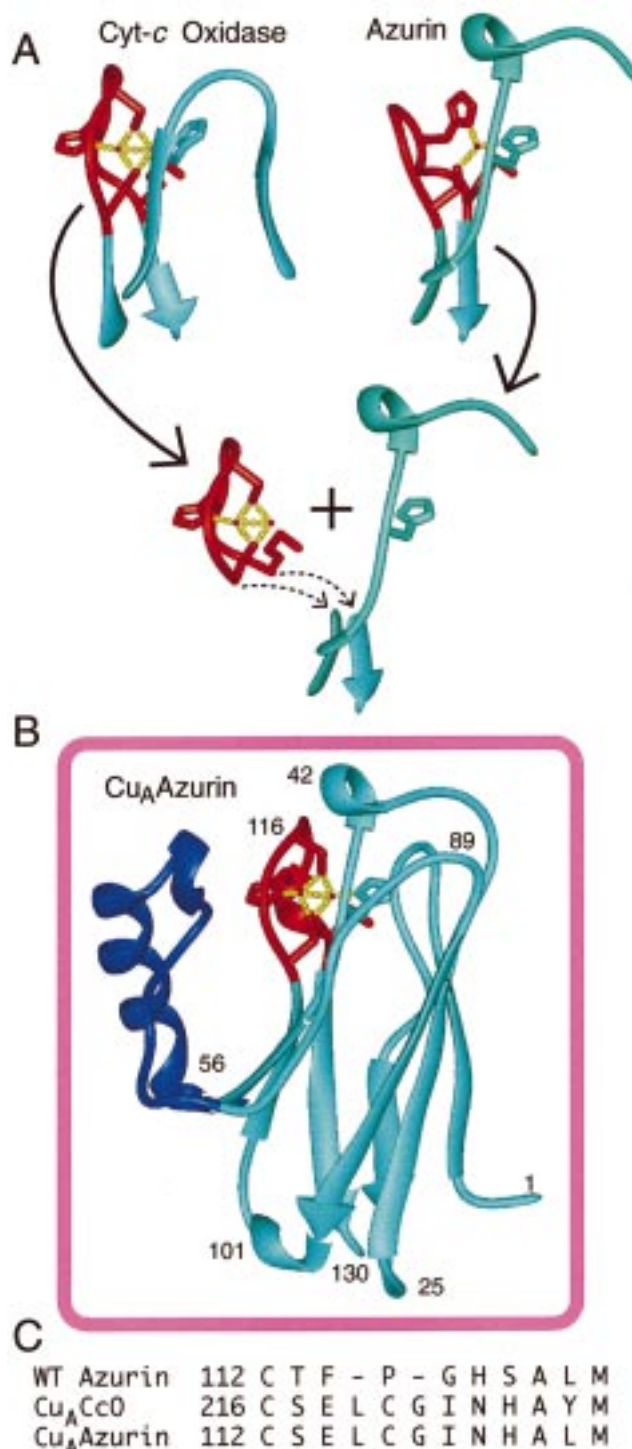


FIGURE 1: (A) Schematic ribbon drawing illustrating the loop-engineered strategy of producing the binuclear purple Cu<sub>A</sub> azurin from the native blue copper azurin. The blue copper binding loop in azurin (amino acids 112–119) is replaced by the Cu<sub>A</sub>-binding loop of COX (*P. denitrificans*) containing the CSELCGINHA sequence as shown in the top panels of the figure. (B) The ribbon diagram of the crystal structure of the purple Cu<sub>A</sub> azurin of molecule A. The other independent molecule B in the asymmetric unit is very similar to molecule A. The ribbon diagram was produced using the algorithm of Kabsch and Sander (53) of MIDAS (University of California, San Francisco).

homogeneity as described previously (37, 43). The loop-engineering strategy is outlined in Figure 1A. The copper binding loop in blue copper azurin is replaced by the Cu<sub>A</sub> binding loop of *P. denitrificans* COX in purple Cu<sub>A</sub> azurin.

Table 1: Crystal and Refinement Data of Cu<sub>A</sub> Azurin

crystal data		refinement data	
<i>a</i> (Å)	35.63	no. of reflections [ $>2.0\sigma(I)$ ] (20–1.65 Å)	23262
<i>b</i> (Å)	62.33	<i>R</i> -factor/ <i>R</i> -free (5% data) [ $>0.0\sigma(I)$ ]	0.201/0.263
<i>c</i> (Å)	51.23	<i>R</i> -factor/ <i>R</i> -free (5% data) [ $>2.0\sigma(I)$ ]	0.189/0.242
$\beta$ (deg)	99.50	rmsd for bond distances (Å)/rmsd for angles (deg)	0.009/2.47
space group	<i>P</i> 2 <sub>1</sub>	no. of protein atoms ( $\langle B \rangle = 11.9 \text{ Å}^2$ )	$2 \times 988$
resolution (Å)	1.65	no. of Cu ions ( $\langle B \rangle = 10.1 \text{ Å}^2$ )	4
no. of reflections [ $>0.0\sigma(I)$ ]	26467	no. of waters ( $\langle B \rangle = 23.8 \text{ Å}^2$ )	506
<i>R</i> <sub>merge</sub> (%)	10.5		
completeness (%)	97.8		
Wilson <i>B</i> -factor (Å <sup>2</sup> )	19.8		

The numbering system of the wild-type blue Cu azurin is used. The amino acids that serve as ligands to Cu ions are bold and underlined. The engineered Cu<sub>A</sub> azurin has a molecular mass of 14 295 Da.

Crystallization was performed by vapor diffusion using 10  $\mu$ L of 23 mg/mL protein in 50 mM ammonium acetate (pH 5.1) and 10  $\mu$ L of a dip solution containing 0.2 M ammonium acetate, 0.1 M sodium acetate (pH 4.6), and 30% polyethylene glycol 2000. The above solution was allowed to equilibrate with 31.5 mL of a reservoir solution containing 0.2 M ammonium acetate, 0.1 M sodium acetate (pH 4.6), and 20% polyethylene glycol 4000 at 5 °C. Purple-colored crystals appeared as clusters of rectangular thin plates. A single 0.2 mm  $\times$  0.4 mm  $\times$  0.05 mm crystal was used for data collection. Data were collected at  $-150$  °C using a Rigaku R-Axis IIc image plate system mounted on an RU-200 rotating-anode X-ray generator (CuK $\alpha$  at 1.5418 Å). The crystal data are listed in Table 1.

The volume of the unit cell (112 217 Å<sup>3</sup>) suggests that there are two Cu<sub>A</sub> azurins in the asymmetric unit, resulting in a reasonable *V*<sub>m</sub> value of 1.96 Å<sup>3</sup>/Da. A self-rotation search indicated that the two molecules are related by an almost-perfect noncrystallographic 2-fold rotational axis with a rotational angle of 179.86°. The structure was solved by the molecular replacement method using X-PLOR (A. Brunger, X-PLOR, version 3.1) (47) using the wild-type azurin structure (PDB file name 4azu) as a search model. The structure was first refined by the simulated annealing procedure as set up in X-PLOR. Subsequently, it was refined by SHELX-97 (48) with individual isotropic temperature factors. Water molecules were then located and added to the refinement using the procedure implemented in SHELX-97 (48). Five hundred six water molecules were located in electron density envelopes at the  $>1.0\sigma$  level. The final *R*-factor for 26 124 reflections [ $>2\sigma(I)$ ] between 20 and 1.65 Å resolution is 0.189. All  $\phi$  and  $\psi$  angles and other protein conformational parameters, calculated by WHAT\_CHECK (49), are within acceptable values. Representative electron density maps, shown in Figure 2, indicate the high-resolution (1.65 Å) nature of the structure. The last shell (1.75–1.65 Å) of the data is 56.4% complete for  $>2.0\sigma(I)$  reflections, and the *R*-factor is 0.355 (Table 1S in the Supporting Information). The final refinement statistics are listed in Table 1. The final atomic coordinates of the two molecules have been deposited at the Brookhaven Protein Data Bank

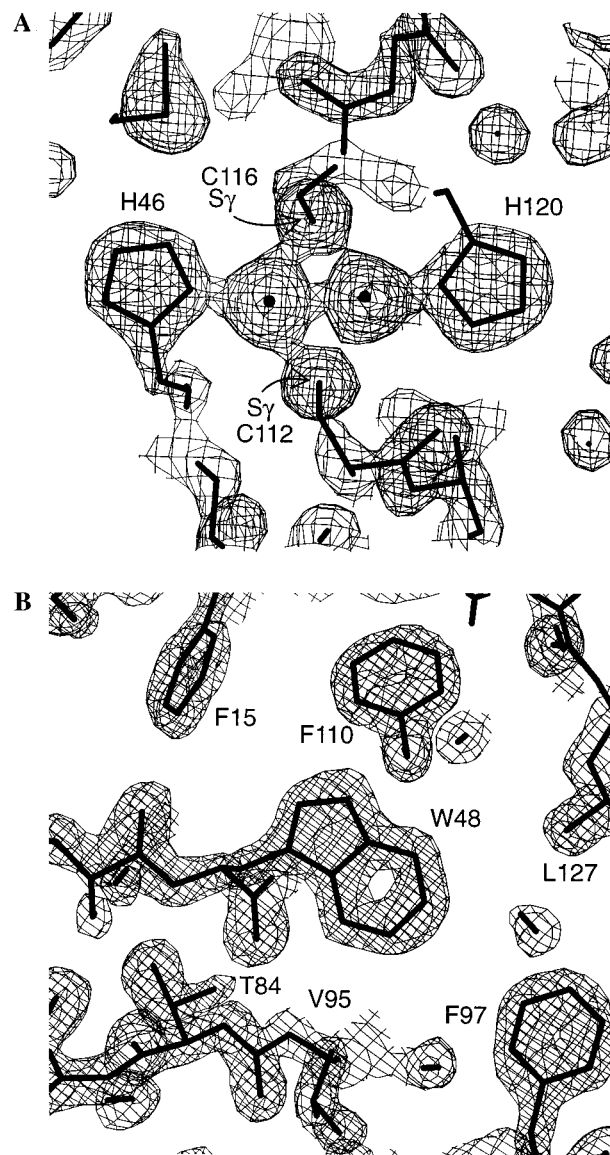


FIGURE 2: (A) The  $2F_o - F_c$  electron density map (contoured at  $2.0\sigma$  level) of the Cu<sub>A</sub> sites at 1.65 Å resolution. The densities of the two copper atoms are well-resolved. The electron density envelope is continuous at the  $1.4\sigma$  level throughout the entire protein backbone of both molecules in the asymmetric unit. (B) The  $2F_o - F_c$  electron density map (contoured at the  $2.0\sigma$  level) of the core region around Trp48.

(file name 1cc3 for the atomic coordinates and r1cc3sf for the structure factor entry).

## RESULTS AND DISCUSSION

**Overall Structure.** There are two independent purple Cu<sub>A</sub> azurin molecules (denoted molecule A and molecule B) in the asymmetric unit of a new *P*2<sub>1</sub> crystal lattice. The two independent purple Cu<sub>A</sub> azurin molecules in the asymmetric unit are very similar to each other, with a root-mean-square deviation (rmsd) of 0.27 Å between them (using all common backbone atoms except residue 1). The overall structure of the Cu<sub>A</sub> azurin (Figure 1B) is nearly identical to the native blue copper azurin. The rmsd of  $\alpha$ -carbon backbones between molecule A and native azurin (PDB file name 4azu) is 0.80 Å when the ligand loop (corresponding to Thr112–Leu120 in the native blue copper azurin) is not considered in the calculation. This result indicates that, as in the case of site-



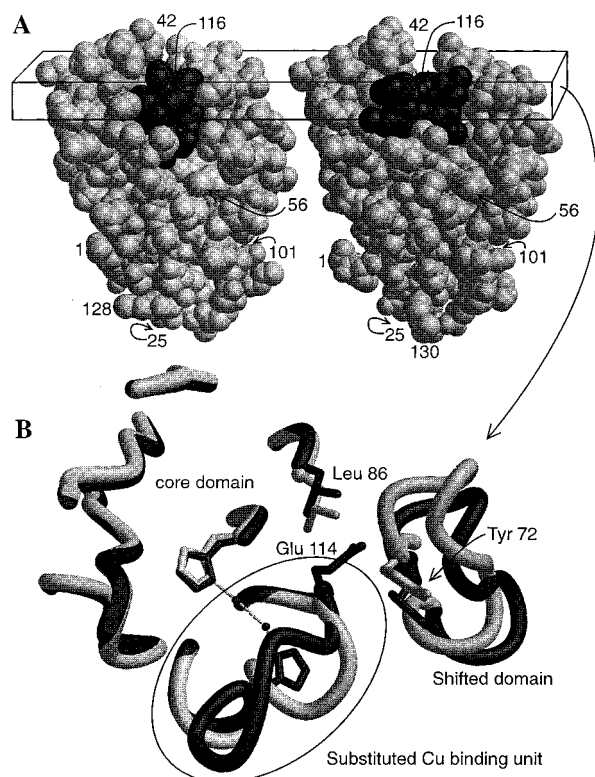


FIGURE 3: (A) van der Waals drawing of the blue copper azurin (left) and  $\text{Cu}_A$  azurin (right). These two drawings are viewed from the side opposite of that in Figure 1B. The Cu-binding loops are shaded. It can be seen that the  $\alpha$ -helix domain is moved to the right side in  $\text{Cu}_A$  azurin. (B) The superposition of the protein protomers that are enclosed by the rectangular box in panel A. The part from the  $\text{Cu}_A$  azurin is darkly shaded, and that from the wild-type azurin is lightly shaded. Note that the part from the  $\beta$ -barrel core domain (located on the left side of the figure) is not shifted, whereas the  $\alpha$ -helix domain is shifted due to the crowding of the side chain from Glu114 of the  $\text{Cu}_A$  loop.

directed mutagenesis, loop-directed mutagenesis does not perturb the overall structure of the protein significantly and new biological activity can be introduced. Consequently, we conclude that this strategy can be generally used in protein engineering.

The newly engineered  $\text{Cu}_A$  azurin crystallizes in a space group ( $P2_1$ ) that is different from that of the wild-type azurin ( $P2_12_12_1$ ). In the crystal of the wild-type azurin, a dimer of dimeric azurins form a tetramer with a pseudo 222 symmetry. The blue Cu centers of azurin are facing toward each other with several amino acids at the protein-protein interface implicated in the electron transfer process. In the  $\text{Cu}_A$  azurin crystal, the purple  $\text{Cu}_A$  center of one azurin is making contacts with the other end of the protein (away from the  $\text{Cu}_A$  center) (Figure 1S in the Supporting Information).

The insertion of a longer loop did result in a hinged movement between the domain loop of residues 52–80 (colored dark blue in Figure 1B) and the main seven-stranded  $\beta$ -barrel body (colored in light blue) of the protein in  $\text{Cu}_A$  azurin which accommodated the larger binuclear  $\text{Cu}_2\text{S}_2(\text{Cys})$  core. The separation of the two parts causes a rearrangement of some amino acid side chains at the interface (Figure 3). Interestingly, the conformation of the loop of Cys112–Met123 is similar between the two independent  $\text{Cu}_A$  azurin molecules (rmsd of 0.20 Å), and to the  $\text{Cu}_A$  site of the native COX from bovine heart (8, 9) and from *P. denitrificans* (10,

11) with respective rmsds of 0.69 and 0.73 Å, respectively.

The conformation of the loop derived from COX is different from that from the blue copper azurin (Figure 1A,B). The insertion of the COX loop places the Glu114 side chain between residues Tyr72 and Leu86. The bulky and negatively charged side chain of Glu114 pushes the  $\alpha$ -helix domain (amino acids 52–82) away from the main  $\beta$ -barrel body (Figure 3B). The newly inserted loop provides most of the Cu-binding ligands, including the  $\text{S}_\gamma$  of Cys112 and Cys116, the  $\text{N}_\epsilon$  of His120, the  $\text{O}_\epsilon$  of Glu114, and the  $\text{S}_\gamma$  of Met123. The remaining ligands are provided by the  $\text{N}_\epsilon$  of His46 and the carbonyl oxygen of Gly45.

**Structure of the Cu-Binding Site.** The two copper atoms in the binuclear  $\text{Cu}_2\text{S}_2(\text{Cys})$  core are completely resolved in the final electron density maps (Figure 2A). The detailed environments at and around the two independent binuclear  $\text{Cu}_2\text{S}_2(\text{Cys})$  cores are shown in Figure 4A. An important finding is that the two independent Cu–Cu distances are 2.42 and 2.35 Å, respectively, shorter than any of the Cu–Cu distances previously observed in  $\text{Cu}_A$  (8–11, 46). There are concomitant changes in the associated Cu–ligand distances.

In molecule A, the  $\text{Cu1–N}^{\text{His46}}$  distance is 2.01 Å and the two Cu– $\text{S}^{\text{Cys}}$  distances are 2.42 and 2.29 Å. In contrast, the  $\text{Cu2–N}^{\text{His}}$  distance is 2.06 Å, and the two Cu– $\text{S}^{\text{Cys}}$  distances are 2.17 and 2.30 Å. In molecule B, the  $\text{Cu1–N}^{\text{His}}$  distance is 2.01 Å and the two Cu– $\text{S}^{\text{Cys}}$  distances are 2.30 and 2.44 Å, whereas the  $\text{Cu2–N}^{\text{His}}$  distance is 2.26 Å and the two Cu– $\text{S}^{\text{Cys}}$  distances are 2.15 and 2.33 Å.

The nonequivalence of the two Cu– $\text{N}^{\text{His}}$  bonds has been noted in both ENDOR (26) and paramagnetic  $^1\text{H}$  NMR (27, 28, 44, 50–52) studies of several  $\text{Cu}_A$  centers. For example,  $^{14}\text{N}$  ENDOR studies of three COXs found that their two nitrogenous ligands have quite different coupling constants, one in the range of 6–11 MHz and the other in the range of 14–17 MHz. Consistent with this observation, a paramagnetic NMR study of purple  $\text{Cu}_A$  amicyanin indicated that the histidine in the ligand loop (His101 in amicyanin, corresponding to His120 here in azurin) has about half of the electron spin density of the other histidine ligand. These results make sense because the Cu– $\text{N}^{\text{His120}}$  bond distance (2.06 Å) is longer than that (2.01 Å) of Cu– $\text{N}^{\text{His46}}$  in molecule A and 2.28 versus 2.08 Å for the respective values in molecule B.

The asymmetry of the  $\text{Cu}_2\text{S}_2$  core has been reflected by the unusually high Cu–S Debye–Waller term in XAS study (24), and by the different chemical shifts of the  $\beta$ - $\text{CH}_2$  protons of the two cysteines (27, 28, 44, 50–52).

For comparisons, the corresponding values of COX from *P. denitrificans* (10, 11) and engineered  $\text{Cu}_A$  in quinol oxidase (CyoA) (46) are shown in panels B and C of Figure 4, respectively. A notable difference among the three  $\text{Cu}_A$  structures is the short Cu–Cu distances (2.42 and 2.35 Å for molecules A and B, respectively) in the  $\text{Cu}_A$  azurin. These distances are consistent with results obtained from EXAFS (2.39 Å) for the same  $\text{Cu}_A$  azurin (42, 43), and are among the shortest Cu–Cu distances in proteins and inorganic complexes. Interestingly, the values in  $\text{Cu}_A$  azurin appear to be more similar to those in COX than to those in  $\text{Cu}_A$  quinoloxidase. In particular, the Cu– $\text{N}_\epsilon$  distances of 1.83 and 1.73 Å in  $\text{Cu}_A$  quinoloxidase are substantially shorter than those (2.01–2.26 Å) of the other two structures. These differences may be responsible for the observation that

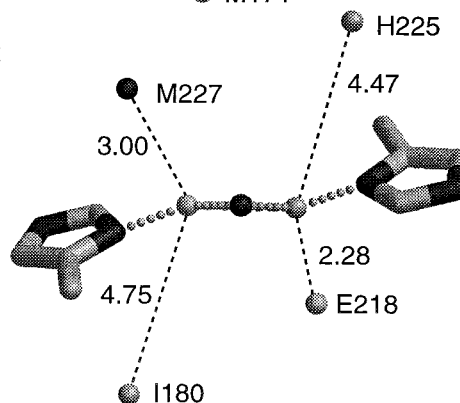
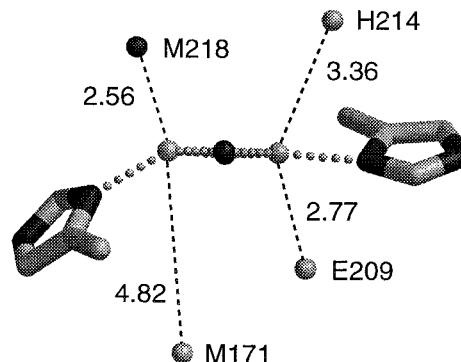
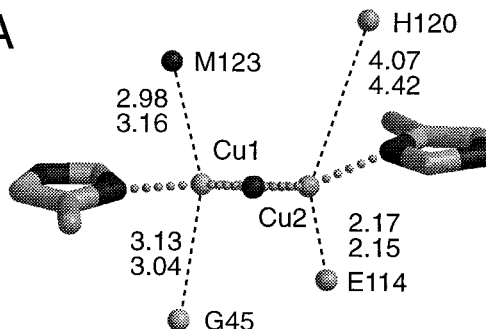
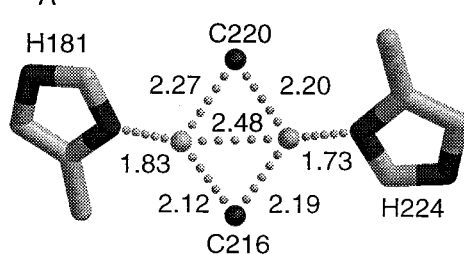
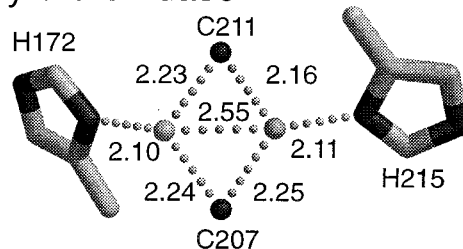
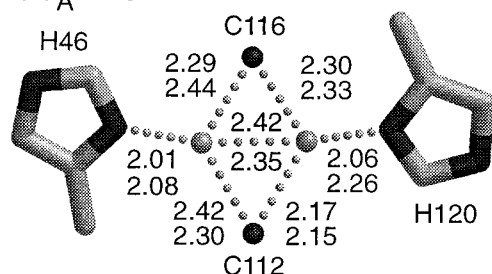


FIGURE 4: Schematic diagram of the Cu<sub>A</sub> site of different Cu<sub>A</sub>-containing proteins, detailing the geometric parameters. (A) In Cu<sub>A</sub> azurin. Numbers in the top and bottom rows are for molecules A and B, respectively. The left view is oriented in a manner similar to that of the electron density map of Figure 2A. The right view is the side view of the Cu<sub>A</sub> site. (B) In COX. (C) In engineered quinol oxidase. The N<sup>His</sup>—N<sup>His</sup> distances for the three structures are 6.33 (molecule A), 6.48, and 5.91 Å, respectively. For axial ligands, sulfur and oxygen atoms are shown with dark and gray shades, respectively.

spectroscopic properties of Cu<sub>A</sub> CyoA are different from those of Cu<sub>A</sub> in native COX (19), while Cu<sub>A</sub> azurin exhibits spectra strikingly similar to those of Cu<sub>A</sub> in native COX (20, 37, 41–43).

In both Cu<sub>A</sub> azurin molecules, the N<sup>His</sup>–Cu–Cu–N<sup>His</sup> line is not straight, and the two N<sup>His</sup> atoms (N<sup>His46</sup> and N<sup>His120</sup>) are slightly out of the binuclear Cu<sub>2</sub>S<sub>2</sub>(Cys) plane by 0.17 and 0.91 Å in molecule A and by 0.04 and 0.56 Å in molecule B, respectively. Deviation of the two N<sup>His</sup> atoms from the Cu<sub>2</sub>S<sub>2</sub>(Cys) plane can also be found in other Cu<sub>A</sub> crystal structures (8–11, 46) (Figure 4B,C, right panels).

A detailed analysis of vibrational data from resonance Raman studies suggested that both histidine nitrogens are removed from the  $\text{Cu}_2\text{S}_2$  plane (21). A detailed electronic spectroscopic characterization and molecular orbital calculations also indicated that the angular position of the histidine nitrogen with respect to the Cu–Cu axis is expected to fine-tune the electronic structure of the  $\text{Cu}_A$  center (20), and therefore its spectroscopic and functional properties.

Weak axial ligand interactions are observed in both molecules, and those interactions are provided by the thioether sulfur of Met123 and the carbonyl oxygens of E114, H120, and G45 (Figure 4A). Similar interactions are found in Cu<sub>A</sub> centers from other proteins (Figure 4B,C). The unique feature of the Cu<sub>A</sub> azurin structure is the relatively shorter distance from the copper to the carbonyl oxygens of E114 (2.17 and 2.15 Å for molecules A and B, respectively) and G45 (3.13 and 3.04 Å for molecules A and B, respectively) than to the corresponding carbonyl oxygens in other Cu<sub>A</sub> structures. The engineered purple Cu<sub>A</sub> from quinol oxidase (purple CyoA) shown in Figure 4C exhibits spectroscopic properties quite different from those of other Cu<sub>A</sub> centers such as native Cu<sub>A</sub> from COX (19). This difference was attributed to the short bond distance (2.28 Å) between the carbonyl oxygen of E218 and Cu in CyoA. However, we found that the corresponding distance in purple Cu<sub>A</sub> azurin is even shorter at 2.15–2.17 Å, yet the purple Cu<sub>A</sub> azurin has been shown to possess spectroscopic properties that are

almost identical to those of native Cu<sub>A</sub> centers (20, 37, 41–43). This shorter distance of the Cu2–E114 bond in Cu<sub>A</sub> azurin may be compensated somewhat by the longer Cu–N<sup>His</sup> distances. Therefore, all four “weak” axial ligand interactions are involved in the maintenance and the fine-tuning of the properties of the Cu<sub>A</sub> center.

*Relationship of the Angular Position of the Histidine Rings and the Axial Ligand Interaction with the Copper Center.* A comparison of the purple Cu<sub>A</sub> azurin structure with those of native Cu<sub>A</sub> in COX from *P. denitrificans* and engineered Cu<sub>A</sub> in CyoA (Figure 4) reveals an important relationship between the angular position of the two N<sup>His</sup> atoms with respect to the Cu<sub>2</sub>S<sub>2</sub>(Cys) core plane and the distance between the Cu and the axial ligand.

The angular position of the two N<sup>His</sup> atoms with respect to the Cu<sub>2</sub>S<sub>2</sub>(Cys) core plane is correlated to the distance between the Cu and the axial ligands. The larger the angle, the longer the distance between Cu and the proximal axial ligand. For example, in the COX structure, the angle between the H172 histidine plane and the Cu<sub>2</sub>S<sub>2</sub>(Cys) core plane is ~30° toward the M171 side. Such an angular position results in a very long Cu1–S<sup>Met171</sup> axial distance (4.82 Å) on the proximal side and a short Cu1–O<sup>Met218</sup> axial distance (2.56 Å) on the distal side. In contrast, the angle between the H215 histidine plane and the Cu<sub>2</sub>S<sub>2</sub>(Cys) core plane is ~0°, resulting in more equal Cu2–O axial distances. Similar observations are found in the other two Cu<sub>A</sub> protein structures.

It has been proposed that both the angular position of the two N<sup>His</sup> atoms with respect to the Cu<sub>2</sub>S<sub>2</sub>(Cys) core plane (20, 21) and the axial ligand interactions with the copper centers (20) are important in fine-tuning the electronic structure and functional properties of the Cu<sub>A</sub> center. Our structure at high resolution provides a firm molecular basis for these contributions. More importantly, our finding of a relationship between the two factors strongly suggests that the fine structural variation of different Cu<sub>A</sub> centers can be described by the angular positions of the two histidine rings because, from these positions, one can predict the relative axial ligand interactions.

## CONCLUSION

In summary, a number of spectroscopic studies using UV–vis absorption, MCD, multifrequency EPR, and EXAFS have argued strongly not only for the similar geometric structures but also for similar bonding characteristics and electronic structures among the Cu<sub>A</sub> centers that have been either isolated from native COX and N<sub>2</sub>OR or engineered from other proteins such as ours. Nonetheless, there are fine structural differences between each member of the purple Cu<sub>A</sub> family, and it is those fine differences that could account for subtle variations in electronic structure and ET function. Our results indicate that the subtle variation occurs between Cu<sub>A</sub> centers of difference proteins. It is remarkable that the engineered purple Cu<sub>A</sub> azurin is rigid enough to impose the rack/entatic state to establish the structure of the purple Cu<sub>A</sub> center yet, at the same time, can be flexible to allow different conformations of the same protein sequence to modulate geometric properties such as the Cu–Cu and ligand–Cu distances and angles.

## ACKNOWLEDGMENT

We thank Priscilla Massey, Angela Kwon, and Xiaotang Wang for help in protein purification.

## SUPPORTING INFORMATION AVAILABLE

One table of crystal data and one figure of crystal packings of azurin and Cu<sub>A</sub> azurin. This material is available free of charge via the Internet at <http://pubs.acs.org>.

## REFERENCES

- Wikström, M., Ed. (1998) Minireview Series: Cytochrome Oxidase: Structure and Mechanism, *Journal of Bioenergetics and Biomembranes*, Vol. 30, Plenum, New York.
- Zumft, W. G., and Kroneck, P. M. H. (1996) *Adv. Inorg. Biochem.* 11, 193–221.
- Malkin, R., and Malmström, B. G. (1970) *Adv. Enzymol.* 33, 177–244.
- Fee, J. A. (1975) *Struct. Bonding (Berlin)* 23, 1–60.
- Ramirez, B. E., Malmström, B. G., Winkler, J. R., and Gray, H. B. (1995) *Proc. Natl. Acad. Sci. U.S.A.* 92, 11949–11951.
- Brzezinski, P. (1996) *Biochemistry* 35, 5611–5615.
- Adman, E. T. (1991) *Adv. Protein Chem.* 42, 145–197.
- Tsukihara, T., Aoyama, H., Yamashita, E., Tomizaki, T., Yamaguchi, H., Shinzawa-Itoh, K., Nakashima, R., Yaono, R., and Yoshikawa, S. (1995) *Science* 269, 1069–1074.
- Tsukihara, T., Aoyama, H., Yamashita, E., Tomizaki, T., Yamaguchi, H., Shinzawa-Itoh, K., Nakashima, R., Yaono, R., and Yoshikawa, S. (1996) *Science* 272, 1136–1144.
- Iwata, S., Ostermeier, C., Ludwig, B., and Michel, H. (1995) *Nature* 376, 660–669.
- Ostermeier, C., Harrenga, A., Ermler, U., and Michel, H. (1997) *Proc. Natl. Acad. Sci. U.S.A.* 94, 10547–10553.
- Beinert, H. (1997) *Eur. J. Biochem.* 245, 521–532.
- Kelly, M., Lappalainen, P., Talbo, G., Haltia, T., van der Oost, J., and Saraste, M. (1993) *J. Biol. Chem.* 268, 16781–16787.
- Speno, H., Taheri, M. R., Sieburth, D., and Martin, C. T. (1995) *J. Biol. Chem.* 270, 25363–25369.
- Zickermann, V., Verkhovsky, M., Morgan, J., Wikstrom, M., Anemuller, S., Bill, E., Steffens, G. C. M., and Ludwig, B. (1995) *Eur. J. Biochem.* 234, 686–693.
- Greenwood, C., Hill, B. C., Barber, D., Eglinton, D. G., and Thomson, A. J. (1983) *Biochem. J.* 215, 303–316.
- Kroneck, P. M. H., Antholine, W. E., Kastrau, D. H. W., Buse, G., Steffens, G. C. M., and Zumft, W. G. (1990) *FEBS Lett.* 268, 274–276.
- Neese, F., Zumft, W. G., Antholine, W. E., and Kroneck, P. M. H. (1996) *J. Am. Chem. Soc.* 118, 8692–8699.
- Farrar, J. A., Neese, F., Lappalainen, P., Kroneck, P. M. H., Saraste, M., Zumft, W. G., and Thomson, A. J. (1996) *J. Am. Chem. Soc.* 118, 11501–11514.
- Gamelin, D. R., Randall, D. W., Hay, M. T., Houser, R. P., Mulder, T. C., Canters, G. W., de Vries, S., Tolman, W. B., Lu, Y., and Solomon, E. I. (1998) *J. Am. Chem. Soc.* 120, 5246–5263.
- Andrew, C. R., Fraczekiewicz, R., Czernuszewicz, R. S., Lappalainen, P., Saraste, M., and Sanders-Loehr, J. (1996) *J. Am. Chem. Soc.* 118, 10436–10445.
- Wallace-Williams, S. E., James, C. A., de Vries, S., Saraste, M., Lappalainen, P., van der Oost, J., Fabian, M., Palmer, G., and Woodruff, W. H. (1996) *J. Am. Chem. Soc.* 118, 3986–3987.
- Williams, K. R., Gamelin, D. R., LaCroix, L. B., Houser, R. P., Tolman, W. B., Mulder, T. C., de Vries, S., Hedman, B., Hodgson, K. O., and Solomon, E. I. (1997) *J. Am. Chem. Soc.* 119, 613–614.
- Blackburn, N. J., de Vries, S., Barr, M. E., Houser, R. P., Tolman, W. B., Sanders, D., and Fee, J. A. (1997) *J. Am. Chem. Soc.* 119, 6135–6143.
- Scott, R. A. (1989) *Annu. Rev. Biophys. Biophys. Chem.* 18, 137–158.



26. Gurbiel, R. J., Fann, Y. C., Surerus, K. K., Werst, M. M., Musser, S. M., Doan, P. E., Chan, S. I., Fee, J. A., and Hoffman, B. M. (1993) *J. Am. Chem. Soc.* **115**, 10888–10894.
27. Dennison, C., Berg, A., and Canters, G. W. (1997) *Biochemistry* **36**, 3262–3269.
28. Luchinat, C., Soriano, A., Djinoovic-Carugo, K., Saraste, M., Malmstroem, B. G., and Bertini, I. (1997) *J. Am. Chem. Soc.* **119**, 11023–11027.
29. Morgan, J. E., Jang, D. J., El-Sayed, M. A., and Chan, S. I. (1989) *Biochemistry* **28**, 6975–6983.
30. Oliveberg, M., and Malmström, B. G. (1991) *Biochemistry* **30**, 7053–7057.
31. Winkler, J. R., Malmström, B. G., and Gray, H. B. (1995) *Biophys. Chem.* **54**, 199–209.
32. Regan, J. J., Ramirez, B. E., Winkler, J. R., Gray, H. B., and Malmström, B. G. (1998) *J. Bioenerg. Biomembr.* **30**, 35–39.
33. Lappalainen, P., Aasa, R., Malmström, B. G., and Saraste, M. (1993) *J. Biol. Chem.* **268**, 26416–26421.
34. von Wachenfeldt, C., de Vries, S., and van der Oost, J. (1994) *FEBS Lett.* **340**, 109–113.
35. Slutter, C. E., Sanders, D., Wittung, P., Malmström, B. G., Aasa, R., Richards, J. H., Gray, H. B., and Fee, J. A. (1996) *Biochemistry* **35**, 3387–3395.
36. van der Oost, J., Lappalainen, P., Musacchio, A., Warne, A., Lemieux, L., Rumbley, J., Gennis, R. B., Aasa, R., Pascher, T., Malmström, B. G., and Saraste, M. (1992) *EMBO J.* **11**, 3209–3217.
37. Hay, M., Richards, J. H., and Lu, Y. (1996) *Proc. Natl. Acad. Sci. U.S.A.* **93**, 461–464.
38. Dennison, C., Vijgenboom, E., de Vries, S., van der Oost, J., and Canters, G. W. (1995) *FEBS Lett.* **365**, 92–94.
39. Houser, R. P., Young, J. V. G., and Tolman, W. B. (1996) *J. Am. Chem. Soc.* **118**, 2101–2102.
40. Barr, M. E., Smith, P. H., Antholine, W. E., and Spencer, B. (1993) *J. Chem. Soc., Chem. Commun.*, 1649–1652.
41. Andrew, C. R., Lappalainen, P., Saraste, M., Hay, M. T., Lu, Y., Dennison, C., Canters, G. W., Fee, J. A., Slutter, C. E., Nakamura, N., and Sanders-Loehr, J. (1995) *J. Am. Chem. Soc.* **117**, 10759–10760.
42. Blackburn, N. J., Ralle, M., Sanders, D., Fee, J. A., de Vries, S., Houser, R. P., Tolman, W. B., Hay, M. T., and Lu, Y. (1998) *ACS Symp. Ser.* **692**, 241–259.
43. Hay, M. T., Ang, M. C., Gamelin, D. R., Solomon, E. I., Antholine, W. E., Ralle, M., Blackburn, N. J., Massey, P. D., Wang, X., Kwon, A. H., and Lu, Y. (1998) *Inorg. Chem.* **37**, 191–198.
44. Wang, X., Ang, M., and Lu, Y. (1999) *J. Am. Chem. Soc.* **121**, 2947–2948.
45. Farver, O., Lu, Y., Ang, M. C., and Pecht, I. (1999) *Proc. Natl. Acad. Sci. U.S.A.* **96**, 899–902.
46. Wilmanns, M., Lappalainen, P., Kelly, M., Sauer-Eriksson, E., and Saraste, M. (1995) *Proc. Natl. Acad. Sci. U.S.A.* **92**, 11955–11959.
47. Brünger, A. (1993) *X-PLOR*, version 3.1, The Howard Hughes Medical Institute and Yale University, New Haven, CT.
48. Sheldrick, G. M. (1997) *SHELX-97, crystallographic refinement program*, University of Gottingen, Gottingen, Germany.
49. Hoof, R. W. W., Vriend, G., Sander, C., and Abola, E. E. (1996) *Nature* **381**, 272.
50. Dennison, C., Berg, A., de Vries, S., and Canters, G. W. (1996) *FEBS Lett.* **394**, 340–344.
51. Bertini, I., Bren, K. L., Clemente, A., Fee, J. A., Gray, H. B., Luchinat, C., Malmström, B. G., Richards, J. H., Sanders, D., and Slutter, C. E. (1996) *J. Am. Chem. Soc.* **118**, 11658–11659.
52. Salgado, J., Warmerdam, G., Bubacco, L., and Canters, G. W. (1998) *Biochemistry* **37**, 7378–7389.
53. Kabsch, W., and Sander, C. (1983) *Biopolymers* **22**, 2577–2637.

BI9901634